Research Report

High Performance Lead-free Piezoelectric Material

Yasuyoshi Saito, Hisaaki Takao, Toshihiko Tani, Tatsuhiko Nonoyama, Kazumasa Takatori, Takahiko Homma, Toshiatsu Nagaya, Masaya Nakamura

Abstract

Lead has recently been expelled from many commercial applications and materials (for example, from solder, glass and pottery glaze) owing to concerns regarding its toxicity. Lead zirconium titanate (PZT) ceramics are high-performance piezoelectric materials, which are widely used in sensors, actuators and other electronic devices; they contain more than 60 weight per cent lead. Although there has been a concerted effort to develop lead-free piezoelectric ceramics, no effective alternative to PZT has yet been found.[1-14] Here we report a lead-free piezoelectric ceramic with an electric-field-induced strain comparable to typical actuator-grade PZT. We achieved this through the combination of the discovery of a morphotropic phase boundary in an alkaline niobate-based perovskite solid solution, and the development of a processing route leading to highly <001> textured polycrystals. The ceramic exhibits a piezoelectric constant d_{33} (the induced charge per unit force applied in the same direction) of above 300 picocoulombs per newton (pC N^{-1}), and texturing the material leads to a peak d_{33} of 416 pC N^{-1}. The textured material also exhibits temperature-independent field-induced strain characteristics.

Keywords: Piezoelectrics, Perovskite structure, Pseudo-illmenite structure, Morphotropic phase boundary, Texture orientation, Electric-field induced strain, Templated grain growth, Topochemical reaction

1. Material design

1. 1 Compositional design

The piezoelectric properties of PZT materials can be improved by the formation of a morphotropic phase boundary (MPB) between the tetragonal and rhombohedral phases in solid solutions of perovskite-type $PbTiO_3$ and $PbZrO_3$ (Refs. 15-17). For the development of new, lead-free piezoelectric materials, we designed a compositional formation of MPB between a different pair of crystal structures–namely, the pseudo-ilmenite-type and perovskite-type structures, having rather different lattice forms and unit sizes from each other. We anticipated the formation of a new MPB in the perovskite-rich region by the dissolution of a small amount of the pseudo-ilmenite-structured material, causing a lattice distortion for the structural phase transition. The general need for stable piezoelectric characteristics over a wide temperature range made us select high Curie-temperature (T_C >250 ^oC) end members: orthorhombic perovskite-type $(K_{0.5}Na_{0.5})NbO_3$ (T_C = 415 ^oC) and hexagonal pseudo-ilmenite-type $LiTaO_3$ (T_C = 615 ^oC). Besides the formation of a MPB, we also exploited the hybridization of covalency onto ionic bonding for further improvement in piezoelectricity, on the basis of Cohen's calculation for the titanate-perovskite system.[18] In addition to $LiTaO_3$, we also used $LiSbO_3$ as an end member for the compositional study with $(K_{0.5}Na_{0.5})NbO_3$, because the higher electronegativities of Sb and Ta compared to Nb were expected to make the alkaline niobate-based perovskite more covalent.

Figure 1a shows the result of the MPB study: a phase diagram determined by X-ray diffraction (XRD) measurements at room temperature (25 ^oC) for conventionally sintered and unpoled ceramic specimens, and d_{31} (the induced charge per unit force applied in the perpendicular direction) values for the specimens poled (given a macroscopic polar

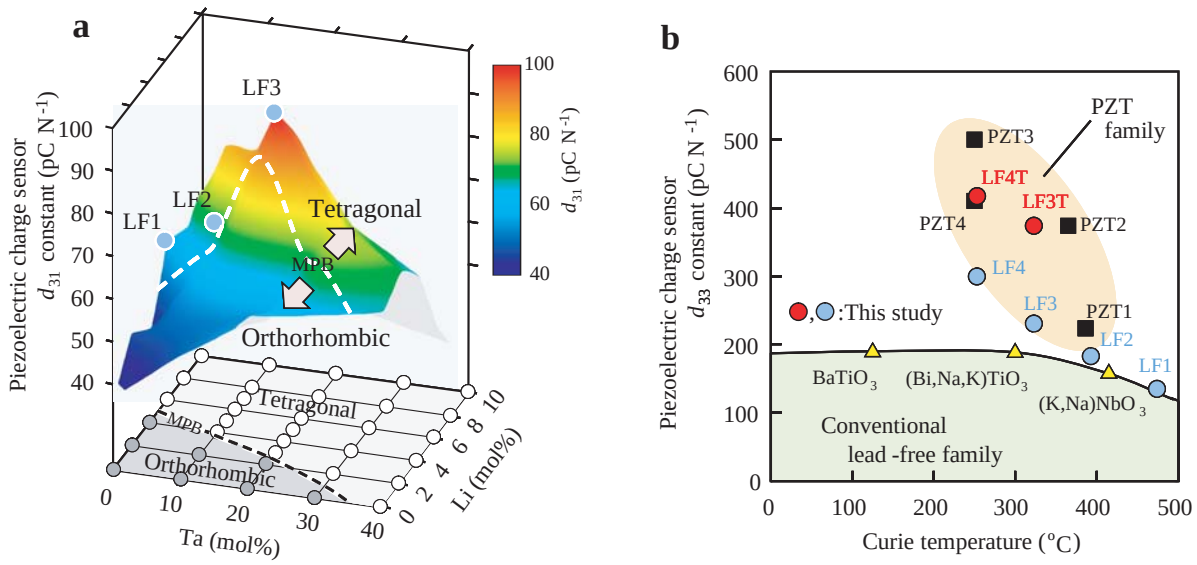

Fig. 1 Piezoelectric sensor performances for the lead-free (LF) piezoelectric ceramics. **a**, Piezoelectric charge sensor d_{31} constants at 25 ^oC as functions of Li and Ta contents for developed $\{(K_{0.5}Na_{0.5})_{1-x}Li_x\}(Nb_{1-y}Ta_y)O_3$ ceramics. The compositions of LF1, LF2 and LF3 are (x, y)=(0.06,0), (x, y)=(0.04,0.10) and (x, y)=(0.03, 0.20), respectively. Note the morphotropic phase boundary (MPB) between tetragonal and orthorhombic phases. The phase diagram was determined by XRD at 25 ^oC for conventionally sintered and unpoled ceramic specimens; d_{31} values are shown for specimens poled at 5 kV mm^{-1}. **b**, Comparison of the piezoelectric charge sensor d_{33} constants at 25 ^oC among developed LF ceramics, previously reported LF ceramics (Refs. 1-3), and conventional PZT ceramics (Refs. 15, 17) as a function of Curie temperature. LF4: $(K_{0.44}Na_{0.52}Li_{0.04})(Nb_{0.86}T_{a0.10}Sb_{0.04})O_3$. LF3T and LF4T: textured ceramics with the same compositions as LF3 and LF4, respectively. PZT1: $Pb(Zr_{0.52}Ti_{0.48})O_3$.
PZT2: $Pb_{0.988}(Zr_{0.48}Ti_{0.52})_{0.976}Nb_{0.024}O_3$. PZT3: commercially available PZT. PZT4: $\{(Pb_{0.85}Ba_{0.15})_{0.9925}La_{0.005}\}(Zr_{0.52}Ti_{0.48})O_3$. The d_{33} values were measured for specimens poled at 5 kV mm^{-1}.

axis by altering the direction of the spontaneous polarization with an applied high electric-field) at 5 kV mm^{-1}.

The compositions with high d_{31} values, shown in Fig. 1 as LF1, LF2 and LF3, are found in a tetragonal phase area near the MPB formed between orthorhombic and tetragonal phases in the alkaline niobate-based perovskite system. The Curie temperature is controllable between 170 and 500 ^{o}C in this compositional range, such that additions of Li and Ta elements shift the Curie temperature higher and lower, respectively. The highest piezoelectric charge sensor d_{33} constant in the (K, Na)NbO_3-$LiTaO_3$ system was found to be 230 pC N^{-1} with a Curie temperature of 323 ^{o}C at the LF3 composition. The introduction of the solid solution in the (K, Na)NbO_3-$LiTaO_3$-$LiSbO_3$ pseudo-ternary system further enhanced the piezoelectric performance, including a d_{33} constant up to as high as 300 pC N^{-1}, with a Curie temperature of 253 ^{o}C (at the LF4 composition, which is also a tetragonal phase at 25 ^{o}C in the unpoled state; Fig. 1b). These excellent piezoelectric properties exceed the d_{33} constant (200 pC N^{-1}) of the non-doped PZT (PZT1 in Fig. 1b).

1. 2 Texture orientation

By additional engineering of the microstructural design, we developed a novel processing route for producing textured polycrystals of the alkaline niobate-based compositions, LF3 and LF4. The d_{33} constants and Curie temperatures are shown in Fig. 1b for the textured ceramics LF3T and LF4T, of which the Lotgering's factors[19] of the <001> orientation are 92% and 91%, respectively. The enhanced d_{33} constants are 373 and 416 pC N^{-1} for LF3T and LF4T, respectively, which are 1.8 and 1.6 times as large as those of non-textured ceramics, LF3 and LF4, respectively.

For the successful fabrication of textured ceramics with high d_{33} values, one of the most important technologies is the preparation of plate-like particles, which are used as a template. The hot-working (hot-forging[20] and hot-pressing[21]) method cannot give a texture to such a pseudo-isotropic system, and no proper template materials have been available for the templated grain growth and reactive-templated grain growth (RTGG)[22-27] of the alkaline niobate-based perovskite. We have developed a new synthesis technique for plate-like $NaNbO_3$ particles as templates for <100> oriented (K, Na)NbO_3-based ceramics. This process comprises three steps as follows: (1) Bismuth layer-structured plate-like $Bi_{2.5}Na_{3.5}Nb_5O_{18}$ ($BiNN_5$) particles (shown in **Fig. 2**b and c) are synthesized as a precursor by the molten-salt synthesis method. (2) Using this precursor, plate-like $NaNbO_3$ particles (Fig. 2d and e), identified by JCPDS powder diffraction file card No.33-1270, are synthesized through a topochemical reaction, in which $NaNbO_3$ is formed by ion exchange of Na for Bi ions on BiNN5 with

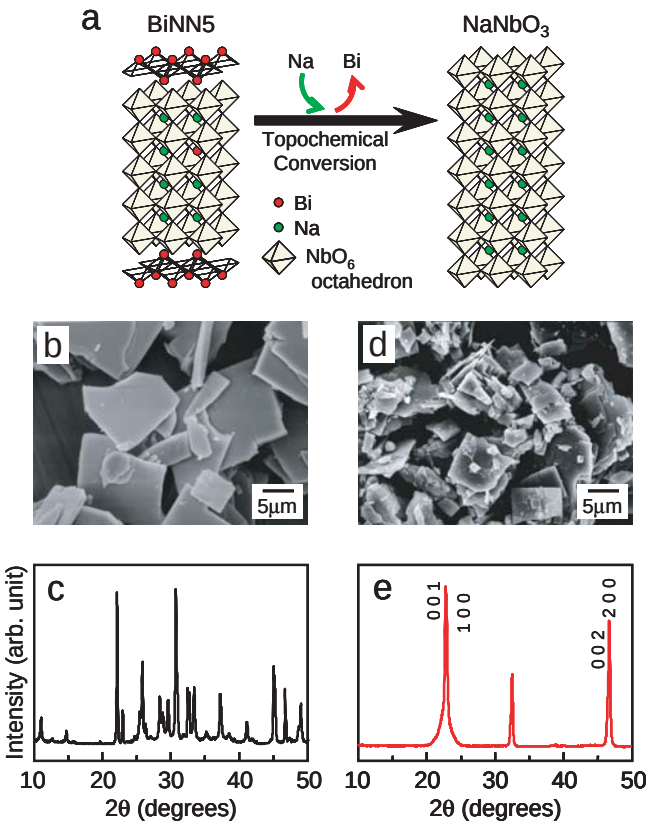

Fig. 2 Schematic diagram of topochemical conversion from bismuth layer-structured BiNN5 particles to plate-like $NaNbO_3$ particles. **a**, Crystal structures of plate-like BiNN5 and $NaNbO_3$ particles. **b**, **c**, SEM image and X-ray diffraction profile of plate-like BiNN5 particles used as precursor. **d**, **e**, SEM image and X-ray diffraction profile of plate-like $NaNbO_3$ particles. X-ray diffraction profile of $NaNbO_3$ particles is characterized by pseudo-tetragonal Miller indices. BiNN5 particles are completely converted into the regular perovskite-structured $NaNbO_3$ particles with a preserved plate-like shape.

preserved particle morphology and a developed {001} plane of the perovskite (Fig. 2a). (3) This $NaNbO_3$ platelet is used as a reactive template, and textured (K,Na)NbO_3-$LiTaO_3$(-$LiSbO_3$) polycrystals are synthesized by the RTGG method.

Figure 3a and b shows the scanning electron micrograph (SEM) image and X-ray diffraction (XRD) profile of textured $(K_{0.44}Na_{0.52}Li_{0.04})(Nb_{0.84}Ta_{0.10}Sb_{0.06})O_3$ ceramic (LF4T) in comparison to those of the non-textured ceramic (LF4) with the same composition. It should be noted that the textured ceramic give brick-layer-like quadrangular grains, which align parallel to the tape-casting plane, and the {001} diffraction peaks of the textured ceramic in the XRD pattern are clearly high compared to those of the non-textured ceramic. In addition, the XRD patterns show that the phases of the textured and non-textured ceramics in the unpoled state are tetragonal at 25 °C. From this result, it is considered that the transformation from a low-temperature orthorhombic phase to a high-temperature tetragonal phase occurs below 25 °C.

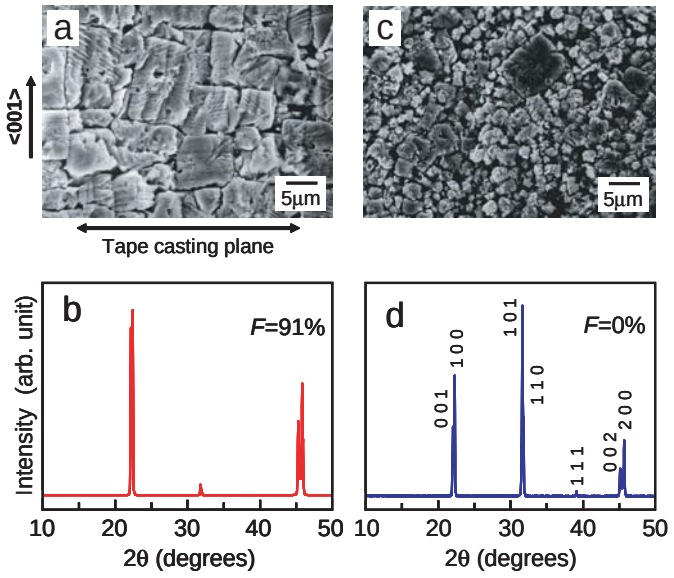

Fig. 3 SEM images of etched cross-sections and X-ray diffraction profiles of textured and non-textured ceramics. **a**, **b**, <001> oriented ceramic (LF4T). The SEM image shows a cross-section perpendicular to the casting plane. **c**, **d**, Non-textured ceramic (LF4) with the same composition as LF4T. *F* denotes the <001> axis orientation factor evaluated by Lotgering's method.

2. Piezoelectric actuator performance

In order to examine the applicability of the developed materials for high-power devices, actuator performances were evaluated. The electric-field-induced strain was measured for the textured LF4T, non-textured LF4 and the conventional PZT ceramic (PZT4) for actuator application under a high electric field from 0 to 2,000 V mm^{-1} with a triangular wave.[28-30)]

For the non-textured LF4 (**Fig. 4**a), the electric-field-induced strain was unstable within this

a

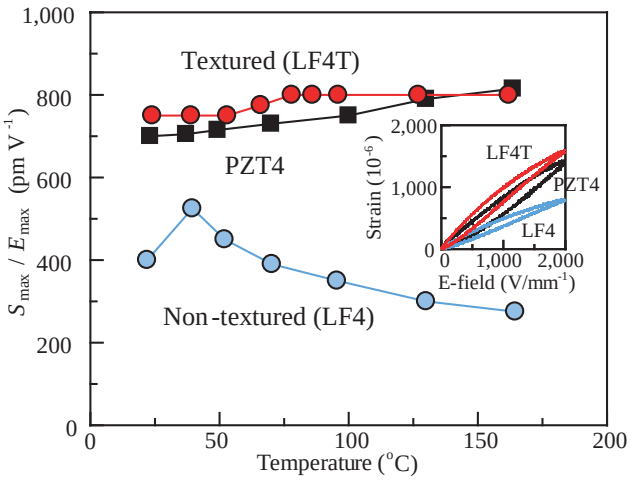

b

Piezoelectric property		LF4T	PZT4
Curie temperature	T_c (°C)	253	250
Piezoelectric coupling constant	K_p	0.61	0.60
Piezoelectric charge sensor constant	d_{31} (pC/N)	152	170
	d_{33} (pC/N)	416	410
Piezoelectric voltage constant	g_{31} (10^{-3} Vm/N)	11.0	8.3
	g_{33} (10^{-3} Vm/N)	29.9	20.2
Dielectric constant	$\varepsilon_{33}^T/\varepsilon_0$	1570	2300
Normalized strain	S_{max}/E_{max} (pm/V)	750	700

Fig. 4 Actuator performances of the developed lead-free piezoelectric ceramics. **a**, Temperature dependences of electric-field-induced longitudinal strain for the textured (LF4T) and non-textured (LF4) ceramics. Inset, electric-field-induced strain curve for LF4T and LF4 at 25 °C. S_{max} and E_{max} denote the maximum strain and the maximum electric field strength, respectively. **b**, Piezoelectric properties of LF4T and PZT4. Dielectric constants were measured at 1 kHz.

temperature range, and had an anomaly: the highest value occurred at 40 ^{O}C. It is considered that this anomaly is related to the electric-field-induced tetragonal-to-orthorhombic phase transformation, shifting the phase transformation temperature from below 25 ^{O}C in the unpoled specimen to 40 ^{O}C under a high electric field. In order to clarify the origin of this anomaly, morphotropic phases need to be determined under high electric-field driving. However, this evaluation is very difficult to perform, and is left for future studies.

On the other hand, it is obvious in Fig. 4a that the textured LF4T, which is the <001> orientated ceramic, exhibited a large strain nearly double of that of the non-textured LF4 ceramic, and the strain was even larger than the field-induced strain for PZT4. In addition, we discovered that the texture given to LF4 not only enhanced the field-induced strain but also improved the temperature coefficient of normalized strain (S_{max}/E_{max}), as shown in Fig. 4a, where S_{max} and E_{max} denote the maximum strain and the maximum electric field strength, respectively. That is to say, the texture stabilizes the temperature-dependent strain characteristic of LF4T, even though its transformation temperature between orthorhombic and tetragonal phases is the same as that of non-textured LF4 in the unpoled state. Furthermore, it should be noted that the flat, temperature-independent characteristic of LF4T is even more prominent than PZT4, since the strain deviation value of 6.5% for LF4T between RT to 160 ^{O}C is smaller than that of 15% for PZT4. This piezoelectric strain behaviour of LF4T is of great importance for temperature-independent actuator devices.

The temperature-independent strain characteristics (for a given texture) are the result of changes in the amplitude of, and in the ratio between, two strain components; one from a lattice motion and the other from domain wall motion.[28-30] Those two field-induced strain components must be dependent on temperature and microstructure (that is, textured or non-textured). In order to clarify the underlying mechanism, a measurement system needs to be developed for the separate evaluation of strain components from the two different origins.

3. Conclusions

The overall performance of the developed LF4T ceramic is listed in Fig. 4b with that of the typical high-performance PZT ceramic (PZT4). It is clear that most of the piezoelectric properties are comparable to those of the PZT. This high performance leads us to expect that the developed materials are leading candidates for environmentally friendly piezoelectric devices.

Supplement: Methods

$Bi_{2.5}Na_{3.5}Nb_5O_{18}$ (BiNN5) platelet was synthesized at 1100 ^{O}C using a molten salt as a flux. $NaNbO_3$ platelet was synthesized in a flux at 950 ^{O}C, and Bi_2O_3, by-product, was removed. The $NaNbO_3$ platelets as reactive templates and complementary reactants, equiaxed $NaNbO_3$, $KNbO_3$, $KTaO_3$, $LiSbO_3$ and $NaSbO_3$ particles, were mixed, tape-cast and stacked. The textured $(K_{0.44}Na_{0.52}Li_{0.04})(Nb_{0.84}Ta_{0.10}Sb_{0.06})O_3$ polycrystal was prepared by sintering the stacked tape at 1135 ^{O}C.

The piezoelectric d_{31} constants were measured by the resonance anti-resonance method with an impedance analyzer (Agilent, HP4194A). The piezoelectric d_{33} constants were measured by the converse piezoelectric method using a piezo-d_{33} meter (Institute of Acoustic Academia Sinica, model ZJ-4B). The degree of tetragonal <001> axis orientation, F, was evaluated by the Lotgering's equation using the X-ray diffractometer (Rigaku, Rint TTR2, CuKα radiation).

Acknowledgements

We thank T. Takeuchi for technical contributions to the development of the processing; T. Saito for discussions; and N. Watanabe, M. Uoshima, H. Morisaka, Y. Aoki, K. Horibuchi, K. Hisazato, M. Okumura, M. Okano, K. Nomura and S. Tsuru for technical assistance.

References

1) Haertling, G. E. : "Ferroelectric Ceramics: History and Technology", J. Am. Ceram. Soc., **82**(1999), 797-818
2) Takenaka, T. and Nagata, H. : "Present Status of Non-lead-based Piezoelectric Ceramics", Key Eng. Mater. **157/158**(1999), 57-64
3) Jaeger, R. E. and Egerton, L. "Hot Pressing of Potassium-sodium Niobates", J. Am. Ceram. Soc., **45**(1962), 209-213

4) Dungan, R. H. and Golding, R. D. : "Polarization of $NaNbO_3$-$KNbO_3$ Ceramic Solid Solutions", J. Am. Ceram. Soc., **48**(1965), 601
5) Haertling, G. H. : "Properties of Hot-pressed Ferroelectric Alkali Niobate Ceramics", J. Am. Ceram. Soc., **50**(1967), 329-330
6) Egerton, L. and Bieling, C. A. : "Isostatically Hot-pressed Sodium-potassium Niobate Transducer Material for Ultrasonic Devices", Ceram. Bull., **47**(1968), 1151-1156
7) Aurivillius, B. : "Mixed Bismuth Oxides with Layer Lattices" Ark. Kemi, **1**(1949), 499
8) Wood, A. : "Polymorphism in Potassium Niobate, Sodium Niobate, and other ABO_3 Compounds", Acta Crystallogr., **4**(1951), 353-362
9) Buhrer, C. F. : "Some Properties of Bismuth Perovskites", J. Chem. Phys., **36**(1962), 798-803
10) Nitta, T. : "Properties of Sodium-lithium Niobate Solid Solution Ceramics with Small Lithium Concentrations", J. Am. Ceram. Soc., **51**(1968), 626-629
11) Scot, B. A., Giess, E. A., Burns, G. and O'Kane, D. F. : "Alkali-rare Earth Niobates with the Tungsten Bronze-type Structure", Mater. Res. Bull., **3**(1968), 831-842
12) Hellwege, K.-H., Hellwege, A. M., Mitsui, T. and Nomura, S. (eds) : "Numerical Data and Functional Relationships in Science and Technology", New Series, Group 3: Crystal and Solid State Physics, Vol.16, Ferroelectrics and Related Substances Subvol. a, Oxides, (1981), Springer, Berlin
13) Mitsui, T. and Nakamura, E. : "Numerical Data and Functional Relationships in Science and Technology" New Series, Group 3: Crystal and Solid State Physics, Vol.28, Suppl. and Extension to Vol.16, Ferroelectrics and Related Substances Subvol. a, Oxides, (1990), Springer, Berlin
14) Takenaka, T. and Nagata, H. : in Program Summary and Extended Abstract of the 11th US-Japan Seminar on Dielectric and Piezoelectric Ceramics, (2003), 237-244, (US-Japan seminar committee, Sapporo, Hokkaido, Japan, September 9-12)
15) Jaffe, B., Roth, R. S. and Marzullo, S. : "Properties of Piezoelectric Ceramics in the Solid-solution Series Lead Titanate Zirconate-lead Oxide: Tin Oxide and Lead Titanate-lead Hafnate", J. Res. Natl. Bur. Stand., **55**(1955), 239-254
16) Zhang, S. J., Randall, C. A. and Shrout, T. R. : "High Curie Temperature Piezocrystals in the $BiScO_3$-$PbTiO_3$ Perovskite System", Appl. Phys. Lett., **83**(2003), 3150-3152
17) Jaffe, B., Cook, W. R. and Jaffe, H. : Piezoelectric Ceramics, (1971), Academic Press Limited, New York
18) Cohen, R. E. : "Origin of Ferroelectricity in Perovskite Oxides", Nature, **358**(1992), 136-138
19) Lotgering, F. K. : "Topotactical Reactions with Ferrimagnetic Oxides Having Hexagonal Crystal Structures - I", J. Inorg. Nucl. Chem., **9**(1959), 113-123
20) Takenaka, T. and Sakata, K. : "Grain Orientation and Eectrical Properties of Hot-forged $Bi_4Ti_3O1_2$ Ceramics", Jpn. J. Appl. Phys., **19**(1980), 31-39
21) Kimura, T., Yoshimoto, T., Iida, N., Fujita, Y. and Yamaguchi, T. : "Mechanism of Grain Orientation during Hot-pressing of Bismuth Titanate", J. Am. Ceram. Soc., **72**(1989), 85-89
22) Watanabe, H., Kimura, T. and Yamaguchi, T. : "Sintering of Platelike Bismuth Titanate Powder Compacts with Preferred Orientation", J. Am. Ceram. Soc., **74**(1991), 139-147
23) Brahmaroutu, B., Messing, G. L., Trolier-Mckinstry, S. and Selvaraj, U. : in Proc. 10th IEEE Int. Symp. on Applications of Ferroelectrics, Vol. 2 (eds. Kulwicki, B., Amin, A. and Safari, A.) 883-886, (Institute of Electrical and Electronic Engineers (IEEE), (1996), Piscataway, NJ
24) Horn, J. A., Zhang, S. C., Selvaraj, U., Messing, G. L. and Trolier-McKinstry, S. : "Templated Grain Growth of Textured Bismuth Titanate" : J. Am. Ceram. Soc., **82**(1999), 921-926
25) Tani, T. : "Crystalline-oriented Bulk Ceramics with a Perovskite-type Structure", J. Korean Phys. Soc., (Suppl. Iss.), **32**(1998), S1217-S1220
26) Takeuchi, T., Tani, T. and Saito, Y. : "Piezoelectric Properties of Bismuth Layer-structured Ferroelectric Ceramics with a Preferred Orientation Processed by the Reactive Templated Grain Growth Method", Jpn. J. Appl. Phys., **38**(1999), 5553-5556
27) Sugawara, T., Shimizu, M., Kimura, T., Takatori, K. and Tani, T. : "Fabrication of Grain Oriented Barium Titanate", Ceram. Trans., **136**(2003), 389-406
28) Saito, Y. : "Measurement of Complex Piezoelectric d_{33} Constant in Ferroelectric Ceramics under High Electric Field Driving", Jpn. J. Appl. Phys., **34**(1995), 5313-5319
29) Saito, Y. : "Measurement System for Electric Field-induced Strain by Use of Displacement Magnification Technique", Jpn. J. Appl. Phys, **35**(1996), 5168-5173
30) Saito, Y. : "Hysteresis Curve of X-ray Diffraction Peak Intensity in Lead Zirconate Titanate Ceramics, Jpn. J. Appl. Phys, **36**(1997), 5963-5969

Reprinted with permission from NGP Nature Asia Pacific (Nature, 432-7013(2004), 84-87).

Yasuyoshi Saito
Research fields : Ferroelectric materials
Academic society : Ceram. Soc. Jpn., Jpn. Soc. Appl. Phys., Soc. Discrete Variational Xα
Awards : The Richard M. Fulrath Award, 2005

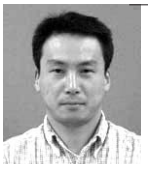

Hisaaki Takao
Research fields : Inorganic materials, Microelectronics technology
Academic degree : Dr. Eng.
Academic society : Jpn. Inst. Met., Jpn. Inst. Electron. Packag.
Awards : Best Research Awards, Jpn. Welding Soc., Microjoining Research Division, 1995
Paper Awards, MATE (Microjoining Assem. Technol. Electron.), 1999
R&D 100 Awards, 2003
Best Research Awards, Ceram. Soc. Jpn., Electronics Division Meeting, 2005
Ceram. Soc. Jpn. Awards for Advancements in Industrial Ceramic Technology, 2006

Toshihiko Tani
Research fields : Synthesis and texture engineering of functional ceramics
Academic degree : Ph. D.
Academic society : Ceram. Soc. Jpn., Am. Ceram. Soc., Jpn. Soc. Appl. Phys., Jpn. Soc. Powder Powder Metall., Mater. Res. Soc. Jpn.
Awards : Jpn. Soc. Powder Powder Metall. Award for Innovatory Research, 2002
Ceram. Soc. Jpn. Award for Academic Achievements, 2005
Dr. Tani concurrently serves as a professor of Toyota Technological Institute.

Tatsuhiko Nonoyama*
Research fields : Ferroelectric materials
Academic degree : Dr. Sci.
Academic society : Phys. Soc. Jpn., Ceram. Soc. Jpn., Jpn. Inst. Met.

Kazumasa Takatori
Research fields : Inorganic material
Academic degree : Dr. Eng.
Academic society : Ceram. Soc. Jpn.

Takahiko Homma
Research fields : Inorganic material
Academic society : Ceram. Soc. Jpn., Electrochem. Soc. Jpn.

Toshiatsu Nagaya*
Research fields : Piezoeleciric materials
Academic society : Soc. Automot. Eng. Jpn.

Masaya Nakamura*
Research fields : Ferroelectric materials
Academic society : Phys. Soc. Jpn.

*DENSO Corp.